Aerosol Science & Technology

ISSN: 0278-6826 (Print) 1521-7388 (Online) Journal homepage: https://www.tandfonline.com/loi/uast20

Passive Aerosol Sampler. Part I: Principle of Operation

Jeff Wagner & David Leith

To cite this article: Jeff Wagner & David Leith (2001) Passive Aerosol Sampler. Part I: Principle of Operation, Aerosol Science & Technology, 34:2, 186-192, DOI: 10.1080/027868201300034808

To link to this article: https://doi.org/10.1080/027868201300034808

Published online: 30 Nov 2010.

Aerosol Science and Technology 34: 186–192 (2001)

Published by Taylor and Francis
0278-6826/01/$12.00 + .00

Passive Aerosol Sampler. Part I: Principle of Operation

Jeff Wagner and David Leith
University of North Carolina, Department of Environmental Sciences and Engineering, Chapel Hill, North Carolina

A method has been developed to estimate average concentrations and size distributions with a miniature passive aerosol sampler. To use the passive sampler, one exposes it to an environment for a period of hours to weeks. The passive sampler is intended to monitor ambient, indoor, or occupational aerosols and has potential utility as a personal sampler. The sampler is inexpensive and easy to operate and is capable of taking long-term samples to investigate chronic exposures. After sampling, the passive sampler is covered and brought to the lab. Scanning electron microscopy (SEM) and automated image analysis are used to count and size collected particles with $d_p > 0.1$ μm. Alternatively, more advanced microscopy techniques can be used for ambient-pressure analysis or elemental characterization. Image analysis is used in conjunction with particle density and shape factors to obtain the mass flux as a function of aerodynamic diameter. The flux and a deposition velocity model are then used to estimate the average mass concentration and size distribution over the sampling period. The deposition velocity model consists of a theoretical component and an empirical component. The theoretical component incorporates gravitational, inertial, and diffusive mechanisms, but can be approximated by the simple terminal settling velocity in many cases. This article, Part I, describes how measurements are made with the passive sampler. The sampler design, theoretical component of the deposition velocity model, and microscopy methods are presented. Part II describes wind tunnel experiments performed to measure sampler precision and determine the empirical component of the deposition velocity.

INTRODUCTION

Epidemiological studies have shown a relationship between particle exposure and community health effects (e.g., Dockery et al. 1993; Thurston et al. 1994; Pope et al. 1995). The causal mechanisms in this relationship are not yet clear, partly due to uncertainties in exposure assessment. In occupational and indoor environments, the threat posed by specific aerosol toxins is better understood, but many aerosol exposures remain uncharacterized.

Received 13 April 1999; accepted 10 December 1999.

Address correspondence to Jeff Wagner, University of North Carolina, Department of Environmental Sciences and Engineering, CB#7400, Rosenau Hall, Chapel Hill, NC 27599. E-mail: jrwagner@lbl.gov

Current techniques to assess aerosol exposures have limitations. For example, long-term chronic exposures are often estimated by averaging several short-term samples. Obtaining a reliable average with this approach is difficult, however, because short-term levels may vary over time or be autocorrelated (Rappaport 1994). Mean exposure can also be assessed with a continuous monitor, but power and maintenance requirements make this method relatively expensive.

Another problem is the large number of samplers needed for some types of exposure studies. Monitoring community exposure with a few centrally-located samplers may not adequately represent exposures in outlying regions (Liu et al. 1995). Similarly, multiple samplers are required to represent the exposure variability between individuals in heterogeneous populations. Many samplers are also needed to investigate the relationship between indoor, outdoor, and total personal exposure levels (Suh et al. 1992). These tasks can be costly and labor intensive if conventional pump-operated samplers are used.

Although personal samplers are typically much smaller than stationary samplers, their sampling pumps can be noisy, heavy, or bulky. This issue is important because any inconvenience experienced by a person wearing a personal sampler may alter behavior and produce nonrepresentative exposure estimates (Wiener and Rodes 1993).

This paper presents a miniature passive aerosol sampler that can be used to estimate long-term average size distributions and concentrations. The passive sampler is intended to monitor ambient, indoor, or occupational aerosols over a period of hours to weeks and has the potential to be used as an area monitor or as a personal sampler. The longer sampling times of the passive sampler should improve assessments of long-term mean exposures. The sampler is cheaper and easier to operate than conventional samplers and therefore a larger number of passive samplers can be deployed. Because the passive sampler is much lighter, smaller, and quieter than pump-operated personal samplers, it may yield more representative measurements.

During sampling, particles passively deposit on the sampler's collection surface. Afterwards, the sampler is enclosed in a plastic case and transported to the lab for analysis using scanning electron microscopy (SEM). Alternatively, more advanced

microscopy techniques can be used for ambient-pressure analysis or elemental characterization. During SEM analysis, collected particles with $d_p > 0.1$ μm are representatively counted and sized and elemental compositions can be determined as well. The resulting flux measurement (particles collected/(area-time)) and a semiempirical deposition velocity model are then used to determine the average concentration and size distribution to which the sampler was exposed.

Previous investigators have raised concerns about passive sample collection, noting that particle deposition is dependent on wind speed and particle size (Lehtimaki and Willeke 1993). Indeed, simply examining the deposited particles without considering the physics of the particle deposition will lead to highly uncertain and distorted size distribution calculations. For this reason, the present work incorporates a deposition velocity model that calculates particle deposition as a function of both particle size and turbulence level.

The passive sampler developed in this research differs from the designs of previous investigators in several respects. The passive dust monitor of Brown et al. (1995) collects particles electrostatically with a charged electret. Calculation of aerosol concentration requires knowledge of the average aerosol electrical mobility and electret charge. Alternatively, electret mass can be correlated with the results of conventional samplers (Brown et al. 1996). The passive sampler of Vinzents (1996) collects particles onto upward-facing, sideways-facing, and downward-facing substrates. A light extinction technique can be used to provide an index of mass concentration. The sampler of Vinzents measures approximately 14 cm × 6 cm × 5 cm, somewhat larger and heavier than the passive sampler of this research.

This article begins with a brief description of the sampler design. The sampling and analysis procedures for the passive sampler are then described, including the theoretical basis of the deposition velocity model and the microscopy methods. Part II describes tests conducted on the passive sampler using a specially-designed wind tunnel (Wagner and Leith 2001).

SAMPLER DESIGN

The design objectives for this research were to create a passive sampler that is small and lightweight, sturdy, convenient for microscopy analysis, and resistant to sample contamination or resuspension. A schematic of the passive sampler is shown in Figure 1. The body of the sampler is composed of either an aluminum or carbon SEM sample mount. Aluminum-based samplers are preferable for size distribution analyses because their high conductivity allows for good resolution. Carbon-based samplers are preferable when elemental analysis is important to minimize interference with the elemental spectra. A 1.5 cm diameter cap supporting a stainless steel mesh is mounted onto the SEM base with spray mount adhesive. The spray mount securely fastens the mesh caps during sampling, but allows removal of the caps afterwards for analysis. The semiquiescent collection region is 1.2 mm deep and 6.8 mm in diameter, and the mesh is 127 μm thick. Because the machining of the SEM substrates often creates microscopic grooves and imperfections, a circular collection surface of smooth aluminum tape is mounted on the "floor" of the collection region. The particles that collect on the smooth substrate can then be analyzed with a minimum of interference.

The purpose of the mesh cover is to prevent deposition of very large particles, such as sand, hair, or other debris, onto the collection surface. The particle sizes that are removed by the mesh are determined by the mesh pore size. A smaller mesh size

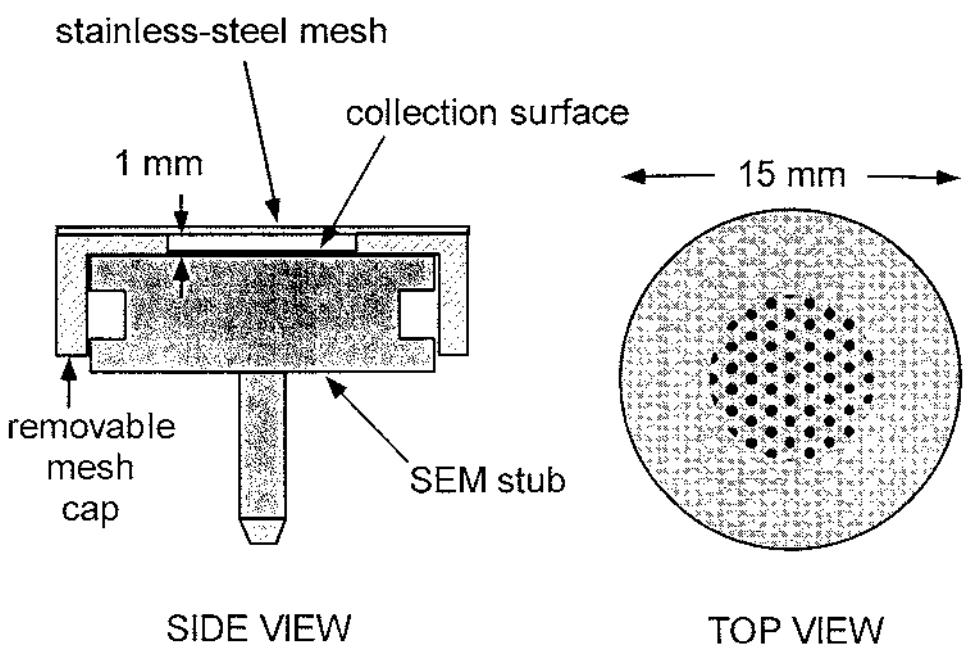

Figure 1. Passive sampler design.

is desirable because it will prevent more unwanted large particles from depositing. However, a smaller mesh size will also collect some smaller particles by diffusion and interception, which will reduce the total sample size. Thus the mesh size was selected to reach a compromise between these two concerns. A mesh with holes of conical cross section and dimensions of 160 μm (top diameter) and 225 μm (bottom diameter) has been selected for general use (Buckbee-Mears, St. Paul, Inc.). However, a range of mesh sizes is commercially available and can be selected with respect to the sampling application.

DEPOSITION VELOCITY MODEL

Several particle deposition models have been described in the literature for various applications, including studies of atmospheric dry deposition, particle deposition in microelectronic clean rooms, smog chamber wall losses, and indoor air deposition (e.g., Sehmel and Hodgson 1978; Slinn and Slinn 1980; Liu and Ahn 1987; Nazaroff and Cass 1987; Cooper et al. 1989; Schneider et al. 1994). An expression commonly used in these models is the deposition velocity:

$$v_{dep} = F/C, \qquad [1]$$

where F is the flux of particles to a given surface and C is the bulk aerosol concentration. The deposition velocity, F, and C are all functions of particle diameter.

These models vary in the particle transport mechanisms they consider. For this research, the relevant deposition mechanisms are convective diffusion, inertia, and gravitational settling. Thermophoresis, electrostatic Coulomb forces, and electrostatic image forces have not been included in the model. Any temperature gradients that occur between the sampler surface and the surrounding air are expected to be random and short lived. Therefore the average temperature gradient is assumed to be zero over the several-week sampling period. Similarly, any voltages that accumulate on the sampler are expected to be transient rather than continuous and would be difficult to quantify accurately. Nevertheless, when possible the sampler should be grounded. The magnitude of electrostatic image forces are probably not important compared to the other deposition mechanisms (McMurry and Rader 1985).

A schematic for the deposition velocity model is shown in Figure 2. A collected particle is assumed to travel from the turbulent atmosphere into the passive sampler's boundary layer, through the sampler's mesh holes, into the sampler's collection region, and finally onto the collection surface. Along this path, several factors specific to the sampler and mesh geometry can affect particles' deposition velocities. For one, if the surrounding wind currents have a large horizontal component, particles can be removed on the leading edge of the sampler by inertia, diffusion and interception. In addition, some particles will be removed by the mesh as they pass into the collection region. Even those particles that travel into the mesh holes can be removed by the hole walls due to inertia, diffusion and interception. Once inside the collection region, some particles will deposit on the underside of the mesh and the collection region walls, enhanced by any air circulations induced inside the collection region. Diffusive deposition inside the collection region may also be influenced by the aerosol concentration inside the collection region.

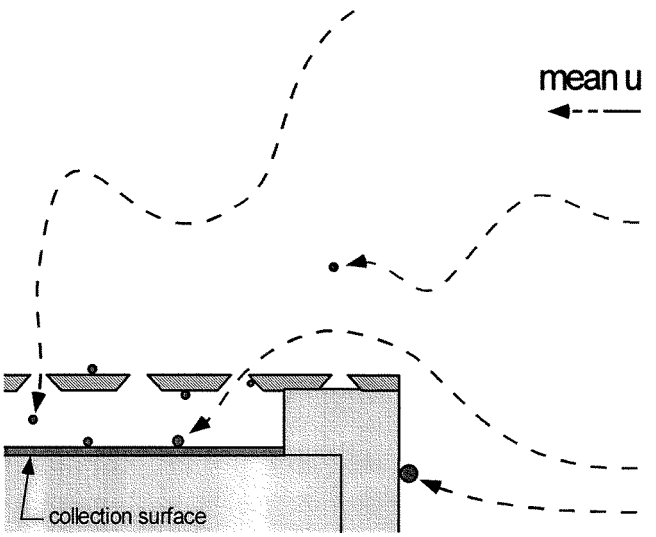

Figure 2. Schematic of deposition into passive sampler with horizontal mean wind velocity.

Expressions analogous to some of these deposition mechanisms have been published in the literature, e.g., enhanced deposition due to surface roughness (Wood 1981), deposition inside a closed vessel (Crump and Seinfeld 1981), and deposition in nucleopore filter holes (Heidam 1981). These expressions apply only loosely to the passive sampler's geometry and flow fields, however, and would require assuming values for the variables which could not be measured directly. Thus using a purely mechanistic equation for the deposition velocity was judged to be inappropriate.

We have adopted an alternative approach, conceptually dividing the overall deposition velocity into two components. The first is the ambient deposition velocity, v_{amb}, which describes the deposition velocity a particle would normally have when depositing onto a flat, smooth surface. This component is expressed as a mechanistic equation. The second component is the "mesh factor," γ_m, an empirical correction which is intended to account for the combined effects of the sampler and mesh, as discussed above. The overall deposition velocity is then expressed as

$$v_{dep} = v_{amb}\gamma_m. \qquad [2]$$

The expression for v_{amb} is obtained using a procedure similar to that used by Shimada et al. (1989) and Schneider et al. (1994). For deposition onto a horizontal surface due to turbulent forces

and gravity, one can set up the steady-state equation

$$F_{amb} = v_{amb}C = (D + D_e)\frac{dc}{dy} + v_t c, \quad [3]$$

where F_{amb} is the mass flux onto the surface, $D(= kTC_c/3\pi\mu d_{es})$ is the Brownian diffusion coefficient, k is the Boltzmann constant, T is the ambient temperature, C_c is the Cunningham correction factor, μ is the dynamic viscosity, D_e is the turbulent eddy diffusion coefficient, c is the concentration at height y above the surface, $v_t(= \tau g)$ is the terminal settling velocity, $\tau = (\rho_0 d_a^2 C_c)/(18\mu)$, ρ_0 is the unit particle density, and g is the gravitational acceleration. The equivalent-surface diameter, d_{es}, is the diameter of a sphere with the same surface area as the particle. The aerodynamic diameter, d_a is the diameter of a unit density sphere with the same settling velocity as the particle.

To integrate Equation (3), the terms can be rearranged and converted into dimensionless form:

$$\int_{c^+_{\sigma+}}^{1} \frac{dc^+}{v^+_{amb} - v_t^+ c^+} = \int_{\sigma+}^{\infty} \frac{dy^+}{D^+ + D_e^+}, \quad [4]$$

where $c^+ = (c/C)$, $v^+_{amb} = (v_{amb}/u_*)$, $v_t^+ = (v_t/u_*)$, $y^+ = (yu_*/\nu)$, $D^+ = (D/\nu)$, $D_e^+ = (D_e/\nu)$, ν is the kinematic viscosity, and u_* is the turbulent friction velocity. Integration is carried out from infinity, where $c^+ = (C/C = 1)$, to a distance from the surface equal to the particle's stop distance, σ. After integrating the left-hand side, one obtains

$$\frac{-1}{v_t^+}[\ln(v^+_{amb} - v_t^+(1)) - \ln(v^+_{amb} - v_t^+(c^+_{\sigma+}))] = I^+, \quad [5]$$

where I^+ denotes the integral on the right-hand side of Equation (4). Rearranging terms yields

$$v^+_{amb} = \frac{v_t^+(1 - c^+_{\sigma+}e^{-v_t^+ I^+})}{1 - e^{-v_t^+ I^+}}. \quad [6]$$

Assuming steady-state, the fluxes at infinity and at σ from the surface are equal. Then

$$c^+_{\sigma+} = \frac{v^+_{amb} \times 1}{v_0^+}, \quad [7]$$

where v_0^+ is the nondimensional velocity of a particle at a distance of σ from the wall. Substituting Equation (7) into Equation (6) and rearranging yields

$$v^+_{amb} = \frac{-v_t^+}{\left[\left(1 - \frac{v_t^+}{v_0^+}\right)e^{-v_t^+ I^+}\right] - 1}. \quad [8]$$

The expression for I^+ can be adapted from the work of Wood (1981):

$$I^+ = \frac{1}{\frac{3\sqrt{3}}{29\pi}Sc^{-2/3} + 6.2 \times 10^{-4}(\tau^+)^2}, \quad [9]$$

where S_c is the Schmidt number $(= \nu/D)$, $\tau^+ = (\tau u_*^2/\nu)$ and the surface is assumed to be smooth.

An empirical expression for v_0^+ was developed by Sehmel (1970):

$$v_0^+ = 1.49(\tau^+)^{-0.49}. \quad [10]$$

Finally, substituting Equation (10) into Equation (8) and converting back to dimensional form yields

$$v_{amb} = \frac{-v_t}{[(1 - 0.67\tau^{0.49}u_*^{-0.02}\nu^{-0.49}v_t)e^{-v_t I}] - 1}, \quad [11]$$

where $I = (I^+/u_*)$ and I^+ is given by Equation (9).

To estimate u_*, one can use the correlation

$$u_* = \frac{u}{\ln\left(\frac{z}{z_0}\right)}, \quad [12]$$

where u is the wind speed at height z above the ground and z_0 is the surface roughness. Various authors have compiled values for z_0 corresponding to different surfaces (e.g., Sehmel 1980; McRae et al. 1982), and u can be estimated by consulting data relevant to the given indoor, workplace, or ambient environment. Depending on the sampling application, these data may include previous measurements conducted at the site, literature results for a similar environment, or public-access meteorological data.

When $u_* < 0.4$ m/s, an important simplification to Equation (11) can be made. Figure 3 is a plot of v_{amb} *vs.* d_a for values of u_* from 0.2 to 0.8 m/s. The figure shows that for $u_* < 0.4$ m/s, the ambient deposition velocity is largely independent of u_* and

$$v_{amb} \cong v_t \quad [13]$$

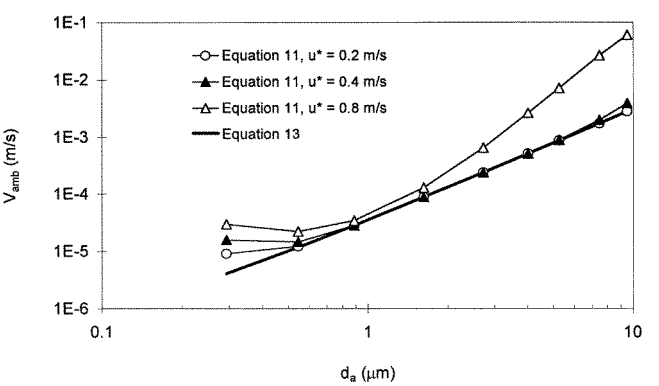

Figure 3. Deposition velocity, v_{dep}, versus aerodynamic particle diameter, d_a, plotted for various friction velocities, u^*.

for $d_a > 0.5\mu$m. The simplification can be assumed to hold for all d_a when calculating PM2.5 and PM10, since these mass metrics usually will be dominated by particles with $d_a > 0.5\ \mu$m.

Equation (13) can be used to approximate Equation (11) in many cases. In U.S. outdoor environments, $u = 4$ m/s (at $z = 10$ m) is a representative wind speed. Using this wind speed and Equation (12), one finds that $u_* < 0.44$ m/s over all surfaces with $z_0 < 2.6$ cm. This z_0 range corresponds to nonurban and nontree-covered areas (McRae et al. 1982). In indoor environments, typical wind speeds are much lower, on the order of $u = 0.1$ m/s. Thus Equation (13) should be applicable in some outdoor and most indoor sampling applications.

The expression for γ_m has been determined experimentally in a wind tunnel:

$$\begin{cases} \gamma_m = 1, & d_a < 1.63\ \mu\text{m}, \\ \gamma_m = (5.95 \times 10^{-3}) Re_p^{-0.439}, & d_a \geq 1.63\ \mu\text{m}, \end{cases} \quad [14]$$

where $Re_p = (d_a v_t/\nu)$. The methods used for this determination are described in detail by Wagner and Leith (2001).

ANALYSIS

After sampling is completed, the passive sampler is transported to the lab in a protective case. In the lab, the case is opened, the mesh cap is removed, and the remaining substrate is then ready for analysis. Analysis of the collected particles can be performed with several different microscopy techniques. Environmental SEM or atomic force microscopy can be utilized to count particles at ambient pressure. With a modified collection substrate, transmission electron microscopy techniques such as cluster analysis, spot-reaction sulfur identification, or EELS spectroscopy could be used (Mamane and de Pena 1978; Saucy et al. 1987; Maynard 1995). An SEM and energy-dispersive x-ray detector were used by Wagner and Leith (2001). SEM is appropriate when the major aerosol constituents are nonvolatile. The energy-dispersive x-ray detector is useful for identifying elements with atomic numbers of 11 and greater. In addition to making an inventory of the elements present in the total collected sample, the chemical compositions of individual particles can be examined in conjunction with their morphology to make inferences about their sources.

To measure the deposition flux as a function of particle size, multiple microscope images are captured by computer at several different magnifications. Fields are selected across the sampler substrate in a random manner, and the particles are semiautomatically counted and sized with the aid of an image analysis software package.

A decision rule is used to count and size particles that are only partially within a given SEM field. Borders of width W, corresponding to the largest particle size expected to be present, are applied to the bottom and right sides of each SEM field. All particles touching these two borders are sized, while all particles touching the other two sides are not. The maximum measurable particle size is then equal to W. At the highest magnifications, W is not allowed to exceed 1/8 of the field height. In addition, a minimum measurable particle size of $d_p = 7$ pixels is set for all magnifications to prevent inaccurate sizing of small particles.

After counting, both the deposition model and count distribution are discretized into size bins. The number and width of size bins is arbitrary; for comparison of results with those from another sampler, one can create size bins that match those of the other sampler. The mass flux for size bin i is then

$$F_i = \frac{N_i \pi (\bar{d}_{ev})_i^3 \rho_p}{6 A_i t}, \quad [15]$$

where N_i is the number of particles counted in size bin i, ρ_p is the particle density, and t is the sampling time. The total field area used for counting, A_i, varies with particle size because for any given magnification, some size bins will not be within measurement limits. For these size bins, the magnification's field area is not counted. The equivalent-volume diameter, d_{ev}, is the diameter of a sphere with the same volume as the particle. The 3rd moment average, $\bar{d}_{ev}$, is used to give the average mass of the size bin:

$$\bar{d}_{ev} = \left[\frac{\int_{(d_{ev})_{i,L}}^{(d_{ev})_{i,h}} d_{ev}^3 dd_{ev}}{\int_{(d_{ev})_{i,L}}^{(d_{ev})_{i,h}} dd_{ev}} \right]^{\frac{1}{3}} = \left[\frac{(d_{ev})_{i,h}^4 - (d_{ev})_{i,L}^4}{4((d_{ev})_{i,h} - (d_{ev})_{i,L})} \right]^{\frac{1}{3}}, \quad [16]$$

where $(d_{ev})_{i,L}$ and $(d_{ev})_{i,h}$ are the lower and upper limits of size bin i.

Because many particles are nonspherical, their sizes are measured in terms of their projected area diameters (d_{pa} is the diameter of a sphere with the same projected area as the particle). The d_{pa} values are then converted to d_{es}, d_{ev}, and d_a. These conversions are made using the following expressions (Davies 1979; Noll et al. 1988):

$$d_{es} = d_{pa} \left(\frac{f}{\pi} \right)^{1/2}, \quad [17]$$

$$d_{ev} = \frac{d_{pa}}{S_v}, \quad [18]$$

$$d_a = d_{ev} \left(\frac{\rho_p C_{c,dev}}{\rho_o C_{c,da}} \frac{1}{S_d} \right)^{1/2}. \quad [19]$$

where f is the surface shape factor, S_v is the volume shape factor, and S_d is the dynamic shape factor. Equations (18) and (19) can be combined to give

$$\frac{d_a}{d_{pa}} = \left(\frac{C_{c,dev}}{C_{c,da}} \right)^{1/2} \left(\frac{\rho_p}{\rho_o} \frac{1}{S_d} \right)^{1/2} \frac{1}{S_v}. \quad [20]$$

Note that for particle sizes $>1\ \mu$m, $C_c \cong 1$ and (d_a/d_{pa}) becomes independent of particle size.

Published data can be used to estimate these parameters (Table 1). Except where indicated, all tabulated values are either measured quantities or are derived from measured quantities.

Table 1
Shape factors and densities for various particle types [D = Davies (1979); C = CRC (1997); S = Stein et al. (1969); N = Noll et al. (1988); L = Lin et al. (1994); H = Hinds (1982)]

Particle type	Ref.	ρ_p (g/cm^3)	S_v	S_d	f	d_a/d_{pa}^a
Common dusts						
Quartz	D	2.65	1.2–1.4	1.36	2.4	0.97–1.16
Sand	D	2.5	1.3	1.57	2.95	1.0
China clay	D	2.2	—	—	—	0.92
Talc	D	2.6	1.5	2.04	2.18	0.73–0.77
Anthracite coal	D	1.5	1.5	1.37	2.2	0.70
Bituminous coal	D	1.4	1.3	1.05–1.11	3.02	0.87–0.90
Glass	D	2.6	—	—	—	1.08–1.34
Cotton	D	1.5	—	—	—	0.72–0.78
Limestone ($CaCO_3$)	C/D	2.7	1.5	—	—	—
Gypsum ($CaSO_4 2H_2O$)	C/D	2.3	1.6	—	—	—
Heterogeneous aerosols						
1969 Pittsburgh aerosol	S	2.2	—	—	—	0.68
1986 Chicago aerosol	N	2.0[b]	1.89	1.41[b]	—	0.63[c]
1992 Chicago aerosol	L	1.77 (fine)[b] 2.64 (coarse)[b]	1.61	1.41[b]	—	0.74[c]
General shapes						
Sphere	H	[1.0]	1.00	1.00	3.14	1.00
Cube	H	[1.0]	1.11	1.02	—	0.89
Compact flake	D	—	1.34	—	2.38	—

[a]For $d_p < 1$ μm, multiply value by (C_{cdev}/C_{cda}).
[b]Estimated, not measured.
[c]Calculated using estimated parameter.

To use Table 1, one must have some knowledge of the aerosol sample's identity. This information can be obtained from the microscopy and x-ray fluorescence. In some cases, the aerosol's composition may be homogenous or well specified, e.g., when sampling in certain industrial environments. In many cases, however, average parameter values must be assumed for a fairly heterogeneous aerosol. For example, a value of $\rho_p = 2.0$ g/cm^3 has been selected as an average value when sampling urban atmospheric aerosols (Noll et al. 1988). Lin et al. (1994) estimated different densities for fine and coarse particles based on their respective primary components, $(NH_4)_2SO_4$ and SiO_2.

Once average aerosol types have been identified, one can consult Table 1 to obtain f, S_v, and S_d. (If Equation (13) is used, d_{es} does not enter into the calculations and f does not need to be estimated.) For particle types with no listed S_v or S_d values, one can calculate d_a directly using the tabulated d_a/d_{pa} values. In contrast with Equation (20), however, these values are not size dependent and are only valid for particle sizes >1 μm. For particles smaller than 1 μm, one should multiply the tabulated value by (C_{cdev}/C_{cda}). Regardless, an estimate of S_v is still required to obtain d_{ev} for use in Equation (15).

To estimate shape factors whose values are not listed in Table 1, one should determine the average shape of the collected particles, i.e., flaky, angular, or rod-like. Then one can estimate S_d or S_v using tabulated values for various particle shapes. Only the most basic shapes are given in Table 1; many more are given by Davies (1979) and Hinds (1982). In addition, procedures exist for calculating S_d for a given geometric shape (Leith 1987) and for agglomerates (Tohno and Takahashi 1990).

Using the mass flux together with Equations (1), (2), (9), and (11) (or Equations (1), (2), and (13) for $u_* < 0.4$ m/s), one can then calculate C for each size bin. The midpoint of each size bin is used to calculate d_{es} in Equation (9). To calculate τ for each size bin $\bar{d}_a$ is used, where

$$\bar{d}_a = \left[\frac{\int_{(d_a)_{i,L}}^{(d_a)_{i,h}} d_a^2 dd_a}{\int_{(d_a)_{i,L}}^{(d_a)_{i,h}} dd_a} \right]^{\frac{1}{2}} = \left[\frac{(d_a)_{i,h}^3 - (d_a)_{i,L}^3}{3((d_a)_{i,h} - (d_a)_{i,L})} \right]^{\frac{1}{2}} \quad [21]$$

and $(d_a)_{i,L}$ and $(d_a)_{i,h}$ are the lower and upper limits of size bin i.

CONCLUSION

A method has been developed to estimate average concentrations and size distributions with a passive aerosol sampler. To use the passive sampler, one exposes it to an environment for a period of hours to weeks. The sampler is then covered and brought to the lab. Microscopy and image analysis are used in conjunction with particle density and shape factors to obtain the mass flux as a function of aerodynamic diameter. The flux and a

deposition velocity model are then used to calculate the average concentration and size distribution to which the sampler was exposed.

The deposition velocity model consists of a theoretical component and an empirical component. The theoretical component incorporates gravitational, inertial, and diffusive mechanisms, but can be approximated by the simple terminal settling velocity in many cases. Wagner and Leith (2001) describe the determination of the empirical component and give the results of laboratory tests of the passive sampler's precision. Field testing is now underway in an occupational environment.

ACKNOWLEDGMENTS

The authors wish to thank the National Institute for Occupational Safety and Health (1 R03 OHO3774-01), the U.S. Environmental Protection Agency (U-915321-01-0), the National Institute of Environmental Health Sciences (5 T32 ES07018-21), the U.S. Department of Education (P200A40274-96), and the UNC Board of Governors for supporting this work.

REFERENCES

Brown, R. C., Hemingway, M. A., Wake, D., and Thompson, J. (1995). Field Trials of an Electret-Based Passive Dust Sampler in Metal-Processing Industries, *Ann. Occup. Hyg.* 39:603–622.

Brown, R. C., Hemingway, M. A., Wake, D., and Thorpe, A. (1996). Electret-Based Passive Dust Sampler: Sampling of Organic Dusts, *Analyst* 121:1241–1246.

Cooper, D. W., Peters, M. H., and Miller, R. J. (1989). Predicted Deposition of Submicrometer Particles Due to Diffusion and Electrostatics in Viscous Axisymmetric Stagnation-Point Flow, *Aerosol Sci. Technol.* 11:133–143.

CRC. (1997). *Handbook of Chemistry and Physics*, 77th Ed., CRC Press, Boca Raton, FL, pp. 15–29.

Crump, J. G., and Seinfeld, J. H. (1981). Turbulent Deposition and Gravitational Sedimentation of an Aerosol in a Vessel of Arbitrary Shape, *J. Aerosol Sci.* 12:405–415.

Davies, C. N. (1979). Particle-Fluid Interaction, *J. Aerosol Sci.* 10:477–513.

Dockery, D. W., Pope, C. A., Xu, X., Spengler, J. D., Ware, J. H., Fay, M. E., Ferris, B. G., and Speizer, F. E. (1993). An Association Between Air Pollution and Mortality in Six U.S. Cities, *N. Engl. J. Med.* 329:1753–1759.

Heidam, N. Z. (1981). Review: Aerosol Fractionation by Sequential Filtration by Nuclepore Filters, *Atmospheric Environment* 15:891–904.

Hinds, W. C. (1982). *Aerosol Technology*, John Wiley and Sons, New York, pp. 48, 365.

Lehtimaki, M., and Willeke, K. (1993). Measurement Methods. In *Aerosol Measurement: Principles, Techniques, and Applications*, edited by K. Willeke and P. A. Baron. Van Nostrand Reinhold, New York, pp. 115.

Leith, D. (1987). Drag on Nonspherical objects, *Aerosol Sci. Technol.* 6:153–161.

Lin, J., Noll, K. E., and Holsen, T. M. (1994). Dry Deposition Velocities as a Function of Particle Size in the Ambient Atmosphere, *Aerosol Sci. Technol.* 20:239–252.

Liu, B. Y. H., and Ahn, K. (1987). Particle Deposition on Semiconductor Wafers, *Aerosol Sci. Technol.* 6:215–224.

Liu, L., Koutrakis, P., Leech, J., and Broder, I. (1995). Assessment of Ozone Exposures in the Greater Metropolitan Toronto Area, *J. Air & Waste Manage. Assoc.* 45:223–224.

Mamane, Y., and DePena, R. G. (1978). A Quantitative Method for the Detection of Individual Submicrometer Size Sulfate Particles, *Atmospheric Environment* 12:69–82.

Maynard, A. D. (1995). The Application of Electron Energy-Loss Spectroscopy to the Analysis of Ultrafine Aerosol Particles, *J. Aerosol Sci.* 26:757–777.

McMurry, P. H., and Rader, D. J. (1985). Aerosol Wall Losses in Electrically Charged Chambers, *Aerosol Sci. Technol.* 4:249–268.

McRae, G. J., Goodwin, W. R., and Seinfeld, J. H. (1982). Development of a Second-Generation Mathematical Model for Urban Air Pollution-I, *Atmospheric Environment* 16:679–696.

Nazaroff, W. W., and Cass, G. R. (1987). Particle Deposition from a Natural Convection Flow onto a Vertical Isothermal Flat Plate, *J. Aerosol Sci.* 18:445–455.

Noll, K. E., Fang, K. Y. P., and Watkins, L. A. (1988). Characterization of the Deposition of Particles from the Atmosphere to a Flat Plate, *Atmospheric Environment* 22:1461–1468.

Pope, C. A., Thun, M. J., Namboori, M. M., Dockery, D. W., Evans, J. S., Speizer, F. E., and Heath, C. W. (1995). Particulate Air Pollution as a Predictor of Mortality in a Prospective Study of U.S. Adults, *Am. J. Respir. Crit. Care. Med.* 151:669–674.

Rappaport, S. M. (1994). Interpreting Levels of Exposures to Chemical Agents. In *Patty's Industrial Hygiene and Toxicology, Third Edition, Volume 3, Part A*, edited by R. L. Harris, L. J. Cralley, and L. V. Cralley. John Wiley and Sons, New York, pp. 349–403.

Saucy, D. A., Anderson, J. R., and Buseck, P. R. (1987). Cluster Analysis Applied to Atmospheric Aerosol Samples from the Norwegian Arctic, *Atmospheric Environment* 21:1649–1657.

Schneider, T., Bohgard, M., and Gudmundsson, A. (1994). A semiempirical Model for Particle Deposition onto Facial Skin and Eyes. Role of Air Currents and Electric Fields, *J. Aerosol Sci.* 25:583–593.

Sehmel, G. A. (1970). Particle Deposition from Turbulent Air Flow, *J. Geophys. Res.* 75:1766–1781.

Sehmel, G. A. (1980). Particle and Gas Dry deposition: A Review, *Atmospheric Environment* 14:983–1011.

Sehmel, G. A., and Hodgson, W. J. (1978). *A Model for Predicting Dry Deposition of Particles and Gases to Environmental Surfaces*, PNL-SA-6721, Batelle, Pacific Northwest Laboratory, Richland, WA.

Shimada, M., Okuyama, K., and Kousaka, Y. (1989). Influence of Particle Inertia on Aerosol Deposition in a Stirred Turbulent Flow Field, *J. Aerosol Sci.* 20:419–429.

Slinn, S. A., and Slinn, W. G. N. (1980). Predictions for Particle Deposition on Natural Waters, *Atmospheric Environment* 14:1013–1016.

Stein, F., Esmen, N. A., and Corn, M. (1969). The Shape of Atmospheric Particles in Pittsburgh Air, *Atmospheric Environment* 3:443–453.

Suh, H. H., Spengler, J. D., and Koutrakis, P. (1992). Personal Exposures to Acid Aerosols and Ammonia, *Environ. Sci. Technol.* 26:2507–2517.

Thurston, G. D., Ito, K., Hayes, C. G., Bates, D. V., and Lippman, M. (1994). Respiratory Hospital Admissions and Summertime Haze Air Pollution in Toronto, Ontario: Consideration of the Role of Acid Aerosols, *Environ. Res.* 65:271–290.

Tohno, S., and Takahashi, K. (1990). Morphological and Dynamic Characterization of Pb Fume Particles Undergoing Brownian Coagulation, *J. Aerosol Sci.* 21:719–732.

Vinzents, P. S. (1996). A Personal Passive Dust Monitor, *Ann. Occup. Hyg.* 40:261–280.

Wagner, J., and Leith, D. (2001). Passive Aerosol Sampler. Part II: Wind Tunnel Experiments, *Aerosol Sci. Technol.* (see subsequent article in this issue).

Wiener, R. W., and Rodes, C. E. (1993). Indoor Aerosols and Aerosol Exposure. In *Aerosol Measurement: Principles, Techniques, and Applications*, edited by K. Willeke and P. A. Baron. Van Nostrand Reinhold, New York, pp. 659–689.

Wood, N. B. (1981). A Simple Method for the Calculation of Turbulent Deposition to Smooth and Rough Surfaces, *J. Aerosol Sci.* 12:275–290.